

# Non-reciprocal Supratransmission in Mechanical Lattices with Non-local Feedback Control Interactions

Jack E. Pechac<sup>1</sup> and Michael J. Frazier<sup>1, a)</sup>

*Department of Mechanical and Aerospace Engineering, University of California, San Diego, California 92093, USA*

(Dated: 22 January 2021)

We numerically investigate the supratransmission phenomenon in an active non-linear system modeled by the 1D/2D discrete sine-Gordon equation with non-local feedback. While, at a given frequency, the typical passive system exhibits a single amplitude threshold marking the onset of the phenomenon, we show that the inclusion of non-local feedback manifests additional thresholds that depend upon the specific boundary from which supratransmission is stimulated, realizing asymmetric (i.e., non-reciprocal) dynamics. The results illustrate a new means of controlling non-linear wave propagation and energy transport for, e.g., signal amplification and mechanical logic.

## I. INTRODUCTION

In the context of elastodynamics, phononic crystals and metamaterials<sup>1,2</sup> – collectively phononic materials – are two classes of materials whose artificial microstructure provides for the management of mechanical waves. For linear, small-amplitude waves, the microstructure design regulates internal scattering and resonance phenomena such that the Fourier components of a disturbance penetrate the material within only particular frequency ranges and in all or specific directions; outside these pass bands, i.e., within the band gaps, wave propagation is prohibited, the associated wave energy decaying exponentially in space. This filtering capability has inspired proposals for a variety of phononic material applications<sup>3–5</sup>. Nevertheless, non-linearities inherent to the microstructure enable a unique dynamic response for large amplitude waves. Supratransmission describes the spontaneous flow of energy within the band gap via the non-linear (non-topological) modes of a medium activated by a boundary driving of sufficient amplitude<sup>6</sup>. The effect is a generic property of non-linear systems, having been shown to emerge from both integrable and non-integrable governing equations<sup>7–12</sup> even when accounting for dissipative effects<sup>13</sup> which more readily extinguish their linear counterparts. This may be exploited, e.g., for the transmission of binary, non-linear signals in lightly-damped systems<sup>14</sup>, as well as for the digital amplification of exceptionally weak signals for sensing<sup>12,15,16</sup>. While these and other studies have promoted an understanding of amplitude-dependent energy transmission, investigations of systems with a directional response, beneficial in applications for greater control of energy flow, are few.

Reciprocity describes the symmetry of wave transmission between two points in space: if a source and receiver exchange positions, the corresponding frequency

response function is identical even in the presence of inhomogeneities and losses<sup>17</sup>. In recent years, inspired by the concept of electric<sup>18</sup> and optical<sup>19,20</sup> diodes and motivated by their application in communications, sensing, and the directional control of energy flow, significant effort has been directed toward the discovery and study of non-reciprocity in other domains of physics. Regarding phononic materials<sup>3,21–24</sup>, inherent non-reciprocity has been demonstrated in a number of systems utilizing unique and intersecting strategies for microstructure design, i.e., internal architectures characterized by internal motion<sup>25</sup>, time-dependent<sup>26–28</sup> and topological<sup>29–31</sup> properties, and non-linearity<sup>32–34</sup>. The focus of these and parallel studies is linear wave manipulation. Transition waves – non-linear (topological) modes characteristic of multi-stable systems which propagate by liberating stored elastic energy – demonstrate non-reciprocity as well<sup>35,36</sup>; however, they are energetically limited to one-time operation or short propagation distances<sup>37</sup>. In the context of supratransmission, Wu *et al.*<sup>38</sup> exploited a spatial asymmetry in the metamaterial construction to elicit non-reciprocal transmission.

While most of the previous references employ a passive material platform, a small but growing collection<sup>25,27,28,30,31,33</sup> investigate linear wave propagation within in an active setting. Recently, feedback control integrated directly into the material architecture has opened the door to more complex interactions unavailable in traditional structures and have been shown to be capable of eliciting non-reciprocal behavior<sup>31,39</sup>. Uniquely, rather than injecting energy into (or extracting from) the system by an external means, feedback involves observing the state of the system and then, following predetermined relations, generating a response that alters the present state. As a result the material behavior is inherent rather than a function of environmental conditions (e.g., temperature, external fields, pumps, actuators which behave independently of the system). At present, the supratransmission phenomenon in feedback mediated non-linear networks has yet to be investigated.

---

<sup>a)</sup>Corresponding author email: mjfrazier@ucsd.edu

In this article, we present an approach to asymmetric (i.e., non-reciprocal) wave propagation in non-linear mechanical networks with a focus on energy transmission within the band gap. Unique in the supratransmission literature, these lattice materials incorporate active elements which impart a local, non-conservative forcing proportional to non-local degrees-of-freedom. The result of this construction is that the onset of the supratransmission phenomenon is not only a function of the driving parameters (i.e., frequency and amplitude) but the specific network boundary at which the excitation is applied and from which wave energy is transmitted to the medium, establishing the asymmetric dynamic behavior.

The article is organized as follows. Section II presents the non-linear governing equation of a representative, one-dimensional mechanical system with feedback and formulates the corresponding dispersion relation of linear, small-amplitude dynamics. In Sec. III, we analyse the supratransmission characteristics of the system, demonstrating asymmetric performance. We also present results for a two-dimensional network. Section IV concludes the article with a summary of the main results and proposals for future research directions.

## II. THEORY

### A. Model

To demonstrate the feedback-mediated asymmetric energy transmission, we initially consider the non-linear dynamics of a one-dimensional (1D) periodic network of coupled pendula, a modified version of that analyzed by Geniet and Leon<sup>6</sup> (Fig. 1a). The pendulum motif is composed of a ring of radius,  $\ell$ , and mass,  $m$ , concentrated at a single point along the circumference. The pendulum rotates (in-plane),  $\varphi$ , about its center which, in the presence a gravitational field of strength  $g$ , adjusts the local potential as  $\psi = mg\ell(1 - \cos \varphi)$ , which describes a non-convex energy landscape responsible for the network non-linearity (Fig. 1b). Moreover, the potential renders the system multi-stable, possessing several energetically degenerate ground states at  $\varphi = 2\pi p$ ,  $p \in \mathbb{Z}$ . Utilizing elastic bands to manifest an effective (torsional) stiffness,  $c = k\ell^2$ , the network emerges via nearest-neighbor coupling. Uniquely, a feedback mechanism imposes an additional, non-conservative influence on each  $\varphi_j$  which, from myriad possible descriptions, we relate to non-local variables; specifically, the torque,  $f_c$ , applied to  $\varphi_j$  via feedback is proportional to the relative rotation of its nearest neighbors, i.e.,  $f_c = s(\varphi_{j+1} - \varphi_{j-1})$ , where  $s$  denotes the proportional control gain. Physically, the feedback mechanism may emerge from active components which sense the non-local displacement and then, through a connected micro-controller and actuator, apply the calculated torque. For example, each pendulum may

connect to a potentiometer which converts the angular displacement to a predetermined voltage drop measured by a programmable micro-controller. Dependent upon the voltage associated with  $\varphi_{j+1}$  and  $\varphi_{j-1}$ , the micro-controller regulates a voltage sent to drive a DC motor which applies a torque,  $f_c$ , to the pendulum at site  $j$ . For an arbitrary pendulum in the 1D network, the non-dimensional governing equation has the form

$$\ddot{\varphi}_j + \bar{c}(2\varphi_j - \varphi_{j+1} - \varphi_{j-1}) + \bar{s}(\varphi_{j+1} - \varphi_{j-1}) + \bar{r} \sin \varphi_j = 0, \quad (1)$$

where  $\bar{c} = c\tau^2/m$ ,  $\bar{s} = s\tau^2/m\ell^2$ , and  $\bar{r} = g\tau^2/m\ell$  are dimensionless parameters. The period of oscillation for an isolated pendulum,  $\tau = 2\pi\sqrt{\ell/g}$ , is a natural choice for the characteristic time and the normalizing parameter defining the dimensionless temporal variable,  $\bar{t} = t/\tau$ . Absent the feedback mechanism (i.e.,  $\bar{s} = 0$ ), Eq. (1) has a form that arises in several domains of science<sup>40-42</sup>; however, the sine-Gordon equation with feedback appears unique to the metamaterial described in this article.

For a system of  $N$  pendula, Eq. (1) forms the basis of a system of equations,  $\mathbf{M}\ddot{\mathbf{u}} + (\mathbf{K} + \mathbf{S})\mathbf{u} + \mathbf{f}_{\text{NL}} = \mathbf{0}$ , where  $\mathbf{M}$ ,  $\mathbf{K}$ , and  $\mathbf{S}$ , respectively, are the mass, stiffness, and feedback matrices;  $\mathbf{u}$  and  $\mathbf{f}_{\text{NL}}$  are, accordingly, the displacement and non-linear force vectors. While the mass and stiffness matrices are symmetric,  $\mathbf{S} \neq \mathbf{S}^T$ , which renders the system non-Hermitian and supportive of non-reciprocal dynamics. Alternatively,  $\mathbf{K} + \mathbf{S}$  may emerge from a system in which the spring interactions, when deformed, manifest unequal forces at each end. Moreover, from the continuum limit of Eq. (1) with expansion  $\varphi_{j\pm 1} \rightarrow \varphi \pm a\varphi_{,x} + a^2\varphi_{,xx}/2$ ,

$$\varphi_{,tt} - \bar{c}a^2\varphi_{,xx} + 2\bar{s}a\varphi_{,x} + \bar{r} \sin \varphi_j = 0,$$

it is apparent that the activity either injects or extracts energy (spatially) from the system depending on the sign of  $\bar{s}\varphi_{,x}$ . Consequently, for a positive  $\bar{s}$  and, e.g., an exponentially decreasing (increasing) displacement function, the active term tends to support (dampen) the motion of  $\varphi$ . Odd spatial derivatives of higher order would have a similar effect.

### B. Dispersion

The proposed system supports a number of amplitude-dependent solutions owing to the non-linear on-site potential. For the particular case of small-amplitude motion, the Fourier components of an initially compact disturbance disperse as the propagation speeds depend on the corresponding wavelength. To establish the dispersion relation, we first linearize Eq. (1) about a (stable) equilibrium configuration and then theoretically extend the pendulum network to infinity through the application of Bloch boundary conditions on a single unit cell; thus, the dynamics of such a

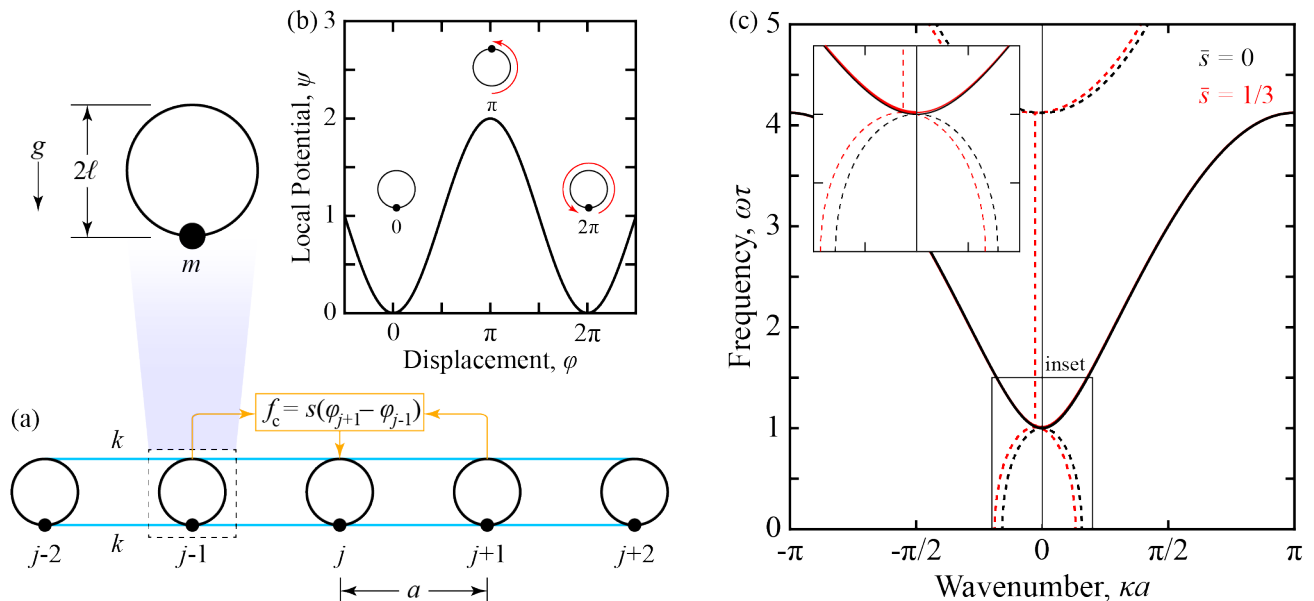


FIG. 1. Pendulum Network with Feedback. (a) One-dimensional network of rotating pendula with elastic bands providing nearest-neighbor coupling and a feedback mechanism imposing a local influence which is proportional to the non-local displacements,  $f_c = s(\varphi_{j+1} - \varphi_{j-1})$ . (b) The on-site, multi-stable potential which manifests the system non-linearity. (c) The complex dispersion of small-amplitude waves of prescribed non-dimensional frequency,  $\omega\tau$ , with real and imaginary wavenumbers,  $\kappa_R$  (solid) and  $\kappa_I$  (dotted), respectively. The feedback effect shifts the attenuating structure about  $\kappa_I = 0$ , provoking non-reciprocal wave propagation.

system are described by  $\varphi_j = \Phi e^{i(\kappa_j a - \omega\tau \bar{t})}$  with  $\kappa$  and  $\omega$ , respectively, the spatial and temporal frequencies. Applied to Eq. (1), the Bloch wave solution entails the following dispersion relation

$$-\omega^2\tau^2 + \bar{c}(2 - \gamma - 1/\gamma) + \bar{s}(\gamma - 1/\gamma) + \bar{r} = 0, \quad (2)$$

where  $\gamma = e^{i\kappa a}$ . The complex band structure emerges from the solution,  $\gamma(\omega\tau)$ , which contains the real and imaginary components of the normalized wavenumber,  $\kappa a = \kappa_R a + i\kappa_I a$ :  $\kappa_R a = \text{Re}[-i\ln(\gamma)]$ , specifying the spatial oscillation of displacement, and  $\kappa_I a = \text{Im}[-i\ln(\gamma)]$ , expressing the spatial attenuation of the amplitude.

### III. RESULTS

#### A. Simulation

In the following, we numerically investigate the dynamics of a representative non-linear network with non-local feedback. To this end, we consider a finite, non-linear system of  $N$  pendula subject to a prescribed harmonic boundary displacement,  $\varphi_j = \Phi \sin(\omega\tau \bar{t})$ , where  $\omega\tau$  is set within the band gap and  $\Phi$  varies between simulations. The left (L) and right (R) boundaries are distinguished, respectively, by  $j = 1$  and  $j = N$ . The system response is quantified by the mean energy transmitted to the network by the driven boundary over

an  $n \in \mathbb{Z}^+$  multiple of the excitation period,  $T$ :

$$E_{\text{in}} = \frac{\bar{c}}{nT} \int_0^{nT} (\varphi_2 - \varphi_1) \dot{\varphi}_1 d\bar{t}, \quad (3)$$

for the left boundary; for the right boundary, substitute the indices in Eq. (3) as  $\{1, 2\} \rightarrow \{N, N - 1\}$ . For sufficiently small amplitudes, the system exhibits a linear response where the energy supplied to the system, ultimately, returns to the driving due to Bragg reflection, causing  $E_{\text{in}}$  to vanish. Conversely, beyond a critical amplitude,  $\Phi_c$ , the driving excites non-linear modes which penetrate the system, resulting in  $E_{\text{in}} > 0$ , signifying a spontaneous energy flow. While a number of methods have been developed to predict the amplitude threshold<sup>7,43-45</sup>, in this article, we intend to introduce the concept of active lattices to the supratransmission literature and initiate exploration of its effects.

Simulations evolve Eq. (1) for a network of  $N = 1000$  coupled pendula with  $\bar{c} = 4$  and  $\bar{r} = 1$  for  $n = 100$  periods. In order to minimize reflections from the free boundary (thus, mimicking an infinite medium), we apply a linearly increasing viscous damping,  $\bar{\eta}\dot{\varphi}_j$ , to the final 800 sites with  $\max(\bar{\eta}) = 1/10$ . In order to avoid the shock wave generated by vanishing initial velocities, the simulations adopt an inaugural velocity profile matching the (linear) evanescent solution at the driving frequency, i.e.,  $\dot{\varphi}_j = -\omega\tau\Phi \cos[(j-1)\kappa_R a]e^{-(j-1)\kappa_I a}$ . In simulation, each boundary is excited in turn, revealing a direction-specific energy transmission for  $\bar{s} \neq 0$ .

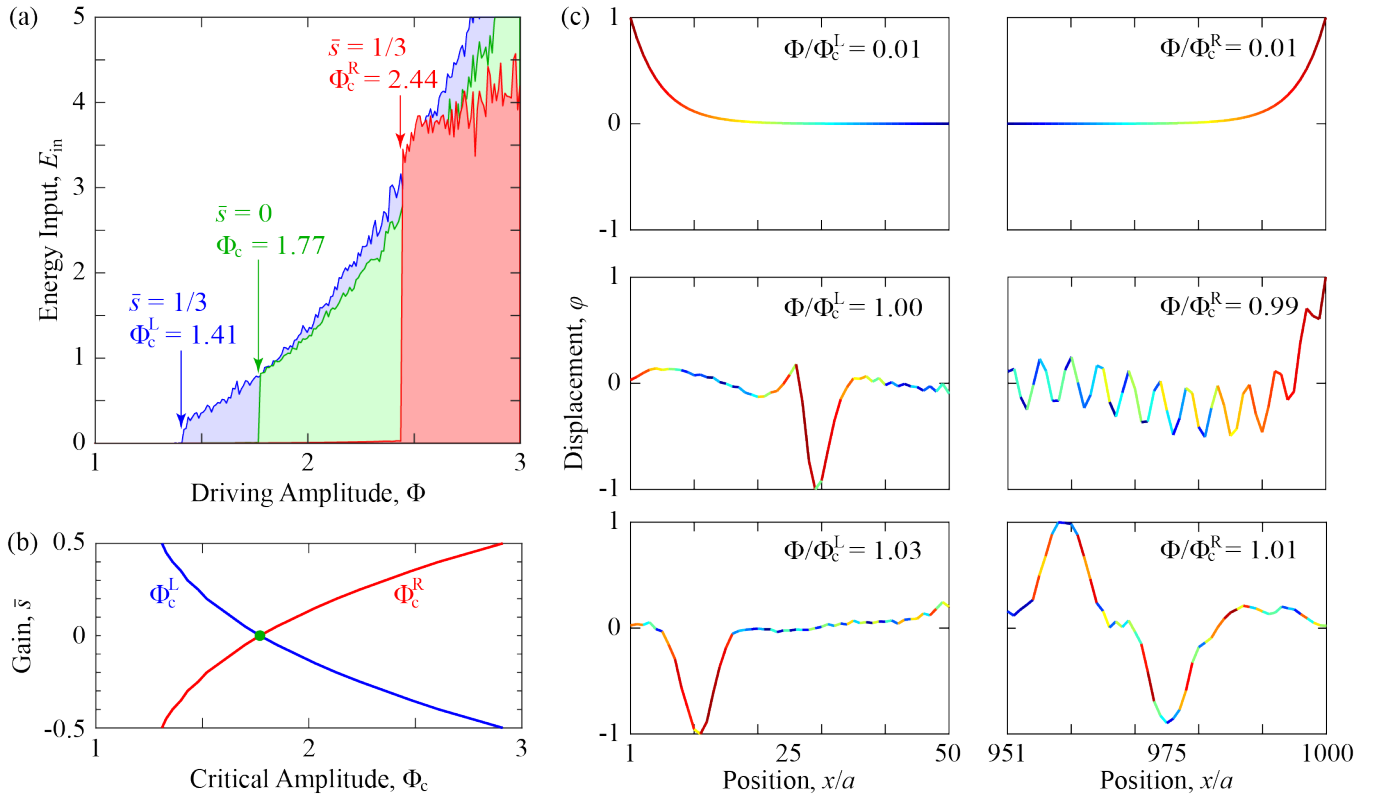


FIG. 2. Asymmetric Supratransmission in One Dimension (color online). (a) Energy transmission as a function of the driving amplitude. For supratransmission, the passive system ( $\bar{s} = 0$ ) exhibits a common threshold amplitude,  $\Phi_c = 1.77$ , when excited from either the left or right boundary; conversely, the active system ( $\bar{s} = 1/3$ ) expresses two thresholds,  $\Phi_c^L = 1.41$  and  $\Phi_c^R = 2.44$ , when excited from the left and right, respectively. (b) The separation of  $\Phi_c^L$  and  $\Phi_c^R$  over a range of  $\bar{s}$ . (c) The normalized displacement profile and energy distribution for an active system ( $\bar{s} = 1/100$ ) at various amplitudes. For each row, the left and right boundaries are subject to the same harmonic excitation, the amplitude of which may be above/below the critical amplitude to trigger supratransmission at the particular boundary.

## B. Supratransmission: One Dimension

Figure 1c graphs the dispersion diagram for instances of passive ( $\bar{s} = 0$ ) and active ( $\bar{s} = 1/3$ ) feedback control, each exhibiting a single pass band separating two band gaps. Apparently, for the reference case where  $\bar{s} = 0$ , the diagram is symmetric about  $\kappa = 0$ , implying that wave propagation is independent of direction. Harmonic boundary driving in the pass band transmits wave energy unabated into the network; in the band gap, Bragg reflection confines energy to the boundary as indicated by  $\kappa_I \neq 0$ . Activating the feedback mechanism modifies the dispersion. While the real component of the band structure,  $\kappa_R(\omega\tau)$ , remains symmetric about  $\kappa = 0$ , the imaginary component,  $\kappa_I(\omega\tau)$ , shifts primarily along the wavenumber axis, breaking the diagram symmetry. This implies that wave propagation, including the supratransmission phenomenon, is direction dependent under non-local feedback control. Analyzing small-amplitude waves, Rosa and Ruzzene<sup>31</sup> also observed non-reciprocal behavior via a feedback effect which was attributed to a complex temporal frequency whose imaginary

component resulted in a propagation direction dependent exponential growth or decay. This article describes a similar effect for non-linear waves which is attributed to a shift in the imaginary wavenumber component of the linear wave dispersion.

Figure 2a plots the energy transmission efficiency of a harmonic boundary driving within the lower band gap ( $\omega\tau = 0.9$ ) in the pendulum network as a function of the driving amplitude for two values of the control gain,  $\bar{s} = 0$  and  $\bar{s} = 1/3$ . In general, below a critical amplitude,  $\Phi_c$ , the linear, small-amplitude response of the system dominates as the total energy remains concentrated near the driven boundary. As the driving amplitude increases, however, higher harmonic modes – the multiples of the driving frequency which appear in the pass band – generated by burgeoning non-linear effects propagate into the system, contributing to a relatively small increase in  $E_{in}$ . For the reference case ( $\bar{s} = 0$ ), beyond the critical amplitude predicted by Geniet and Leon<sup>6</sup>,  $\Phi_c = 1.77$ , the attenuating displacement profile of the linear solution is unstable<sup>46,47</sup>; instead, non-linear modes generated at the driven boundary subsequently propagate into the system, signified by the sudden increase in the transmitted

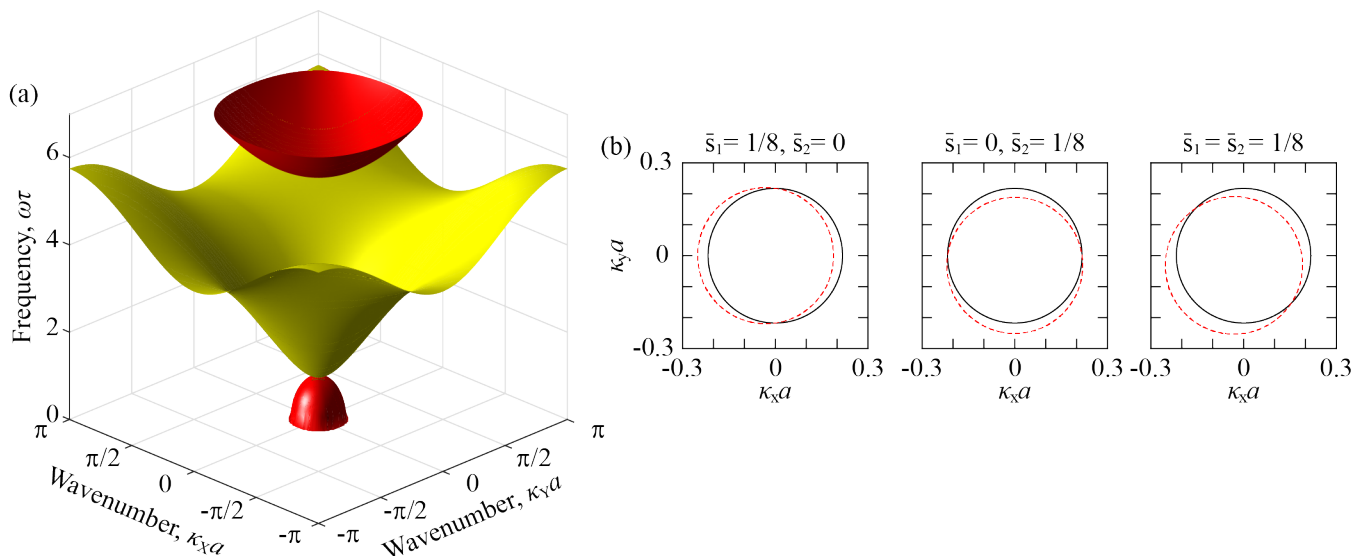


FIG. 3. Dispersion (color online). (a) The complex dispersion surfaces for a passive, square lattice of pendula with near-neighbor interactions, including the propagating (yellow) and attenuating (red) modes. (b) The circular contour formed by the cross-section of the attenuating surface at band-gap frequency  $\omega\tau = 0.9$ . Active feedback, i.e.,  $\bar{s}_{1,2} \neq 0$ , shifts the attenuation contour (red, dashed) with respect to the passive result (black), enabling direction-dependent non-reciprocal wave propagation.

energy, i.e., supratransmission. As the band diagram of the reference system is symmetric (Fig. 1c), the critical amplitude for supratransmission is identical for left- and right-boundary driving. However, setting  $\bar{s} \neq 0$  activates the feedback mechanism and adjusts the band diagram as described previously – for  $\bar{s} = 1/3$  and  $\omega\tau = 0.9$ , forward and backward waves are attenuated according to  $\kappa_{Ia} = 0.150$  and  $\kappa_{IIa} = 0.317$ , respectively – which suggests that  $\Phi_c$  differs for the same excitation on opposite boundaries. The simulation results depicted in Fig. 2a confirm that the amplitude thresholds for supratransmission in the feedback network do, indeed, differ:  $\Phi_c^L = 1.41$  and  $\Phi_c^R = 2.44$ , respectively, for left- and right-boundary driving. Figure 2b shows how the two thresholds diverge as a function of  $\bar{s}$ .

The supratransmission demonstrated in the previous results transmits the energy of a signal with band-gap frequency through a non-linear system. To further emphasize this phenomenon, Fig. 2c displays snapshots of the left and right boundary regions of the active pendula network ( $\bar{s} = 1/100$ ) subject to the same harmonic driving with various amplitudes. For visualization purposes, the instantaneous displacement in the boundary region is normalized such that  $\max(|\varphi_j|) = 1$ . The superposed color indicates the corresponding energy distribution over the same region,  $\mathcal{H}_j = \frac{1}{2}\dot{\varphi}_j^2 + \frac{1}{2}\bar{c}(\varphi_j - \varphi_{j-1})^2 + \psi(\varphi_j)$ . As expected, for small amplitudes, the displacement profile exhibits an exponential decay and energy concentrates at the boundary. In the second row of Fig. 2c, the excitation amplitude exceeds the supratransmission threshold for only the left boundary driving; consequently, the evanescent response is unstable and energy propagates

away from the boundary. The same excitation amplitude does not exceed the critical value for the right boundary; therefore, apart from the aforementioned higher harmonics lying within the pass band, the energy remains localized there.

### C. Supratransmission: Two Dimensions

The pendulum network can be extended to obtain a two-dimensional (2D) periodic system, e.g., a square lattice with nearest-neighbor coupling. Accordingly, the non-local feedback applied to each  $\varphi_{j,k}$  depends on additional terms,  $f_c = \bar{s}_1(\varphi_{j+1,k} - \varphi_{j-1,k}) + \bar{s}_2(\varphi_{j,k+1} - \varphi_{j,k-1})$  where  $\bar{s}_1$  and  $\bar{s}_2$  are gain parameters. Considering a Cartesian frame, indices  $j$  and  $k$  designate sites along the  $x$  and  $y$  axes, respectively, with the indices increasing with the relevant coordinate. Following the same normalization scheme as before, the governing equation for a generic unit cell is

$$\begin{aligned} \ddot{\varphi}_{j,k} + \bar{c}(4\varphi_{j,k} - \varphi_{j+1,k} - \varphi_{j-1,k} - \varphi_{j,k+1} - \varphi_{j,k-1}) \\ + \bar{s}_1(\varphi_{j+1,k} - \varphi_{j-1,k}) + \bar{s}_2(\varphi_{j,k+1} - \varphi_{j,k-1}) \\ + \bar{r} \sin \varphi_{j,k} = 0. \end{aligned} \quad (4)$$

Linearizing Eq. (4) and applying the Bloch solution,  $\varphi_{j,k} = \Phi e^{i(\kappa_x j a + \kappa_y k a - \omega \tau \bar{t})}$ , yields the dispersion relation

$$\begin{aligned} -\omega^2 \tau^2 + \bar{c}(4 - \gamma_x - 1/\gamma_x - \gamma_y - 1/\gamma_y) \\ + \bar{s}_1(\gamma_x - 1/\gamma_x) + \bar{s}_2(\gamma_y - 1/\gamma_y) + \bar{r} = 0, \end{aligned} \quad (5)$$

where  $\gamma_x = e^{i\kappa_x a}$  and  $\gamma_y = e^{i\kappa_y a}$ . Figure 3a plots the complex dispersion surfaces for the passive system

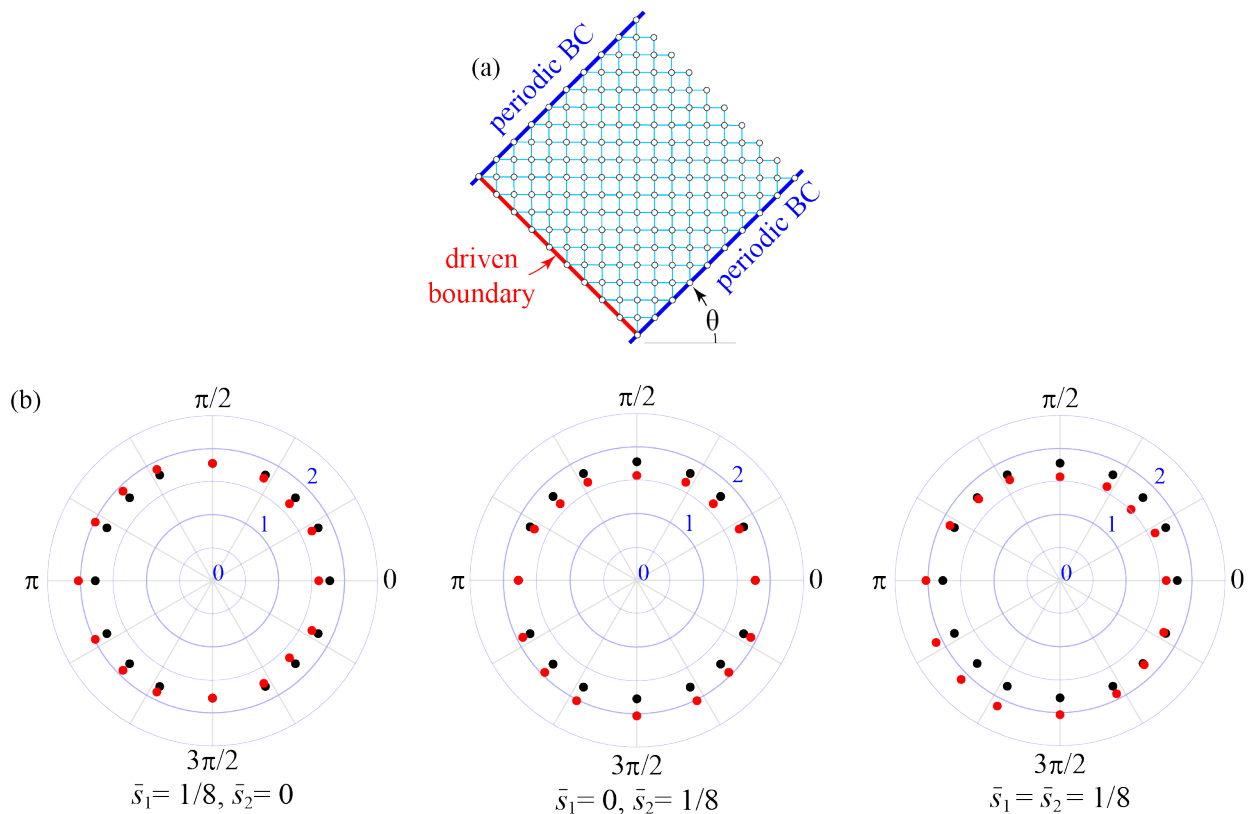


FIG. 4. Asymmetric Supratransmission in Two Dimensions (color online). (a) Finite square lattice with periodic boundary conditions (blue) and a harmonically exciting a line of nodes (red). (b) The threshold amplitude  $\Phi_c$  versus orientation angle  $\theta$  reveals the directional impact of activity for a different combinations of the feedback parameters (red) relative to a passive system (black).

( $\bar{s}_1 = \bar{s}_2 = 0$ ), revealing a single propagating surface separating two attenuating surfaces within frequency band gaps. Since, as before, our focus is in the lower band gap where the real component of the wavevector vanishes, we substitute  $\gamma_x = e^{-\kappa_{I,x}a}$  and  $\gamma_y = e^{-\kappa_{I,y}a}$  in Eq. (5) such that, for a given  $\omega\tau$  in the lower band gap, the  $\kappa_{I,x}$  and  $\kappa_{I,y}$  which satisfy the relation trace the circular contour of the attenuating surface. Specifically, at the band-gap frequency  $\omega\tau = 0.9$ , the diagrams in Fig. 3b compare the attenuating contours of various active systems with that of the passive lattice. Apparently, similar to the earlier 1D system, in the 2D network, activity causes the attenuating contour to shift relative to the passive reference centered at  $(\kappa_x, \kappa_y) = (0, 0)$ , indicating the broken symmetry of the system's small-amplitude dynamics which we expect to persist at larger amplitudes.

To investigate asymmetric supratransmission in the 2D setting, we track the energy transmitted to a square lattice of finite dimension by a set of co-linear sites oscillating in phase at a band-gap frequency (Fig. 4a). Beyond a critical amplitude, the driven boundary generates a wave front which propagates away from the driving and normal to it, i.e., at an angle  $\theta$  with respect to the  $x$ -axis. Thus, the directional dependence of the

supratransmission phenomena may be investigated by adjusting the slope of the driven boundary. To this end, we modify Eq. (3) to accommodate the additional interactions of the 2D system under consideration:

$$E_{\text{in}} = \frac{\bar{c}}{nT} \sum_{m,n} \sum_{r,s} \int_0^{nT} (\varphi_{r,s} - \varphi_{m,n}) \dot{\varphi}_{m,n} d\bar{t}, \quad (6)$$

where  $\{m, n\}$  collects the indices of driven sites and  $\{r, s\}$  the indices of their nearest neighbor(s). Thus Eq. (6) is the time-averaged energy transmitted to the lattice by the driven boundary.

Simulations utilize a square lattice with nearest-neighbor interactions to develop a rectangular system of approximately  $23a \times 800a$  in dimension with the driven sites along one of the smaller dimensions and periodic boundary conditions along the two extended dimensions. For  $\bar{c} = 4$  and  $\bar{r} = 1$ , the excitation frequency  $\omega\tau = 0.9$  lies within the band gap. For  $n = 25$  periods, we evolve the system following Eq. (4) from an initial velocity,  $\dot{\varphi}_{j,k} = -\omega\tau\Phi \cos(\kappa_R d) e^{\kappa_I d}$ , where  $d$  is the perpendicular distance from the driven boundary to the  $(j, k)$ th site and  $\kappa = \kappa_R + i\kappa_I$  is the complex wavenumber in that direction.

For a number of orientations,  $\theta$ , we determine the critical driving amplitude above which  $E_{\text{in}}$  sharply increases. The panels in Fig. 4b display the directional dependence of the threshold amplitude for different combinations of the feedback parameters,  $\bar{s}_1$  and  $\bar{s}_2$ . For the passive system, we determine a  $\theta$ -independent threshold amplitude of  $\Phi_c = 1.77$  which is identical to that of the 1D passive system. However, following the wavenumber contours in Fig. 3b, activity causes the threshold amplitude to shift relative to its passive value, the magnitude of the shift dependent upon  $\theta$ . For the active scenario  $(\bar{s}_1, \bar{s}_2) = (1/8, 0)$ , the minimum amplitude for supratransmission decreases for waves propagating to the right (i.e.,  $|\theta| < \pi/2$ ); increases for waves traveling to the left (i.e.,  $|\theta| > \pi/2$ ). The effect is maximized for  $\theta = 0$  where the wave front aligns with the gradient,  $\varphi_{,x}$ , which determines the strength of  $f_c$ . Conversely, the threshold is unchanged at  $\theta = \pm\pi/2$  where the effect of  $\varphi_{,x}$  and, therefore,  $f_c$  vanish. Figure 4b displays additional orientation-amplitude results for systems with alternative feedback definitions which may be similarly understood.

#### IV. CONCLUSION

To summarize, we numerically investigated the non-linear supratransmission phenomenon in active 1D/2D periodic networks characterized by a non-local feedback control. We found that such a feedback adjusts the imaginary wavenumber component across the whole of the frequency range, although asymmetrically, such that the otherwise reciprocal dynamics becomes direction-dependent. In the context of band gap energy transmission in finite, one-dimensional networks, the critical amplitude for stimulating supratransmission via boundary excitation differs for each boundary. Similarly, for a two-dimensional system, the amplitude threshold changes with boundary orientation. These results demonstrate an alternative, extremely tunable approach toward non-reciprocal dynamics and applications<sup>9,14</sup>.

There are several research directions for subsequent studies. The influence of anisotropy and lattice type, especially those with multiple elements per lattice site (e.g. Lieb, Kagome, etc.), on the directionality of supratransmission is worth investigating. While we have considered a proportional controller with displacement inputs, a natural extension of the present work would explore controllers of derivative- and integral-type to determine the characteristics of each feedback archetype, independently followed by in combination. In addition, feedback definitions involving spatial and temporal rates have yet to be explored.

#### V. ACKNOWLEDGEMENTS

This work is supported by start-up funds provided by the University of California.

- <sup>1</sup>M. I. Hussein, M. J. Leamy, and M. Ruzzene, "Dynamics of phononic materials and structures: historical origins, recent progress, and future outlook," *Appl. Mech. Rev.*, vol. 66, p. 040802, May 2014.
- <sup>2</sup>G. Ma and P. Sheng, "Acoustic metamaterials: From local resonances to broad horizons," *Sci. Adv.*, vol. 2, February 2016.
- <sup>3</sup>X.-F. Li, X. Ni, L. Feng, M.-H. Lu, C. He, and Y.-F. Chen, "Tunable unidirectional sound propagation through a sonic-crystal-based acoustic diode," *Phys. Rev. Lett.*, vol. 106, p. 084301, February 2011.
- <sup>4</sup>J. Zhong, H. Zhao, H. Yang, Y. Wang, J. Yin, and J. Wen, "Theoretical requirements and inverse design for broadband perfect absorption of low-frequency waterborne sound by ultrathin metasurface," *Sci. Rep.*, vol. 9, February 2019.
- <sup>5</sup>I. Benichou and S. Givli, "Force-sensitive metamaterials for vibration mitigation and mechanical protection," *Extreme Mech. Lett.*, vol. 40, October 2020.
- <sup>6</sup>F. Geniet and J. Leon, "Energy transmission in the forbidden band gap of a nonlinear chain," *Phys. Rev. Lett.*, vol. 89, p. 134102, September 2002.
- <sup>7</sup>R. Khomeriki, S. Lepri, and S. Ruffo, "Nonlinear supratransmission and bistability in the Fermi-Pasta-Ulam model," *Phys. Rev. E*, vol. 70, p. 066626, December 2004.
- <sup>8</sup>J. E. Macías-Díaz, "Numerical study of the transmission of energy in discrete arrays of sine-Gordon equations in two space dimensions," *Phys. Rev. E*, vol. 77, p. 016602, January 2008.
- <sup>9</sup>J. E. Macías-Díaz, "Bistability of a two-dimensional Klein-Gordon system as a reliable means to transmit monochromatic waves: a numerical approach," *Phys. Rev. E*, vol. 78, p. 056603, November 2008.
- <sup>10</sup>A. B. Toguet Motchevo, C. Tchawoua, and J. D. Tchingang Tchameu, "Supratransmission induced by waves collisions in a discrete electrical lattice," *Phys. Rev. E*, vol. 88, p. 040901, October 2013.
- <sup>11</sup>B. Yousefzadeh and A. S. Phani, "Energy transmission in finite dissipative nonlinear periodic structures from excitation within a stop band," *J. Sound Vib.*, vol. 354, pp. 180–195, June 2015.
- <sup>12</sup>M. Malishava, "All-phononic amplification in coupled cantilever arrays based on gap soliton dynamics," *Phys. Rev. E*, vol. 95, February 2017.
- <sup>13</sup>F. Geniet and J. Leon, "Nonlinear supratransmission," *J. Phys.: Condens. Matter*, vol. 15, pp. 2933–2949, May 2003.
- <sup>14</sup>J. E. Macías-Díaz and A. Puri, "An application of nonlinear supratransmission to the propagation of binary signals in weakly damped, mechanical systems of coupled oscillators," *Phys. Lett. A*, vol. 366, pp. 447–450, April 2007.
- <sup>15</sup>R. Khomeriki, J. Leon, and D. Chevriaux, "Quantum Hall bilayer digital amplifier," *Eur. Phys. J. B*, vol. 49, pp. 213–218, January 2006.
- <sup>16</sup>M. Malishava and R. Khomeriki, "All-phononic digital transistor on the basis of gap-soliton dynamics in an anharmonic oscillator ladder," *Phys. Rev. Lett.*, vol. 115, p. 104301, September 2015.
- <sup>17</sup>H. Nassar, B. Yousefzadeh, R. Fleury, M. Ruzzene, A. Alu, C. Daraio, A. N. Norris, G. Huang, and M. R. Haberman, "Nonreciprocity in acoustic and elastic materials," *Nat. Rev. Mater.*, vol. 5, September 2020.
- <sup>18</sup>H. Matsuo, Y. Kitanaka, R. Inoue, Y. Noguchi, and M. Miyayama, "Switchable diode-effect mechanism in ferroelectric BiFeO<sub>3</sub> thin film capacitors," *J. Appl. Phys.*, vol. 118, p. 114101, December 2017.
- <sup>19</sup>R. J. Potton, "Reciprocity in optics," *Rep. Prog. Phys.*, vol. 67, pp. 717–754, May 2004.
- <sup>20</sup>T. Kodera, D. L. Sounas, and C. Caloz, "Magnetless nonreciprocal metamaterial (MNM) technology: application

- to microwave components,” *IEEE Transactions on Microwave Theory and Techniques*, vol. 61, pp. 1020–1042, January 2013.
- <sup>21</sup>B. Liang, B. Yuan, and J.-c. Cheng, “Acoustic diode: rectification of acoustic energy flux in one-dimensional systems,” *Phys. Rev. Lett.*, vol. 103, p. 104301, September 2009.
- <sup>22</sup>C. Ma, R. G. Parker, and B. B. Yellen, “Optimization of an acoustic rectifier for uni-directional wave propagation in periodic mass–spring lattices,” *J. Sound Vib.*, vol. 332, pp. 4876–4894, September 2013.
- <sup>23</sup>A. A. Maznev, A. G. Every, and O. B. Wright, “Reciprocity in reflection and transmission: What is a ‘phonon diode’?,” *Wave Motion*, vol. 50, pp. 776–784, June 2013.
- <sup>24</sup>R. Fleury, D. Sounas, M. R. Haberman, and A. Alu, “Nonreciprocal acoustics,” *Acoust. Today*, vol. 11, pp. 14–21, 2015.
- <sup>25</sup>R. Fleury, D. L. Sounas, C. F. Sieck, M. R. Haberman, and A. Alu, “Sound isolation and giant linear nonreciprocity in a compact acoustic circulator,” *Science*, vol. 343, pp. 516–519, January 2014.
- <sup>26</sup>N. Swintek, S. Matsuo, K. Runge, J. O. Vasseur, P. Lucas, and P. A. Deymier, “Bulk elastic waves with unidirectional backscattering-immune topological states in a time-dependent superlattice,” *J. Appl. Phys.*, vol. 118, p. 063103, August 2015.
- <sup>27</sup>Y. Wang, B. Yousefzadeh, H. Chen, H. Nassar, G. Huang, and C. Daraio, “Observation of nonreciprocal wave propagation in a dynamic phononic lattice,” *Phys. Rev. Lett.*, vol. 121, p. 194301, November 2018.
- <sup>28</sup>G. Trainiti, Y. Xia, J. Marconi, G. Cazzulani, A. Erturk, and M. Ruzzene, “Time-periodic stiffness modulation in elastic metamaterials for selective wave filtering: theory and experiment,” *Phys. Rev. Lett.*, vol. 122, p. 124301, March 2019.
- <sup>29</sup>R. K. Pal, M. Schaeffer, and M. Ruzzene, “Helical edge states and topological phase transitions in phononic systems using bi-layered lattices,” *J. Appl. Phys.*, vol. 119, p. 084305, February 2016.
- <sup>30</sup>A. Souslov, B. C. van Zuiden, D. Bartolo, and V. Vitelli, “Topological sound in active-liquid metamaterials,” *Nature Phys.*, vol. 13, pp. 1091–1094, July 2017.
- <sup>31</sup>M. I. N. Rosa and M. Ruzzene, “Dynamics and topology of non-Hermitian elastic lattices with non-local feedback control interactions,” *New J. Phys.*, vol. 22, p. 053004, May 2020.
- <sup>32</sup>B. Liang, X. S. Guo, J. Tu, D. Zhang, and J. C. Cheng, “An acoustic rectifier,” *Nat. Mat.*, vol. 9, pp. 989–992, December 2010.
- <sup>33</sup>B.-I. Popa and S. A. Cummer, “Non-reciprocal and highly nonlinear active acoustic metamaterials,” *Nat. Commun.*, vol. 5, p. 4398, February 2014.
- <sup>34</sup>J. R. Raney, N. Nadkarni, C. Daraio, D. M. Kochmann, J. A. Lewis, and K. Bertoldi, “Stable propagation of mechanical signals in soft media using stored elastic energy,” *Proc. Natl. Acad. Sci.*, vol. 113, pp. 9722–9727, 2016.
- <sup>35</sup>N. Nadkarni, A. F. Arrieta, C. Chong, D. M. Kochmann, and C. Daraio, “Unidirectional transition waves in bistable lattices,” *Phys. Rev. Lett.*, vol. 116, p. 244501, June 2016.
- <sup>36</sup>M. Hwang and A. F. Arrieta, “Solitary waves in bistable lattices with stiffness grading: augmenting propagation control,” *Phys. Rev. E*, vol. 98, p. 042205, October 2018.
- <sup>37</sup>V. Ramakrishnan and M. J. Frazier, “Transition waves in multi-stable metamaterials with space-time modulated potentials,” *Appl. Phys. Lett.*, vol. 117, p. 151901, October 2020.
- <sup>38</sup>Z. Wu, Y. Zheng, and K. W. Wang, “Metastable modular metastructures for on-demand reconfiguration of band structures and nonreciprocal wave propagation,” *Phys. Rev. E*, vol. 97, p. 022209, February 2018.
- <sup>39</sup>M. Brandenbourger, X. Locsin, E. Lerner, and C. Coullais, “Non-reciprocal robotic metamaterials,” *Nat. Commun.*, vol. 10, p. 4608, October 2019.
- <sup>40</sup>Y. I. Frenkel and T. Kontorova, “On the theory of plastic deformation and twinning,” *J. Phys.*, vol. 1, pp. 137–149, 1939.
- <sup>41</sup>J. K. Perring and T. H. R. Skyrme, “A model unified field equation,” *Nuclear Physics*, vol. 31, March 1962.
- <sup>42</sup>B. D. Josephson, “Supercurrents through barriers,” *Adv. Phys.*, vol. 14, pp. 419–451, 1965.
- <sup>43</sup>G. Kopidakis and S. Aubry, “Discrete breathers and delocalization in nonlinear disordered systems,” *Phys. Rev. Lett.*, vol. 84, pp. 3236–3239, April 2000.
- <sup>44</sup>Z. Wu and K.-W. Wang, “On the wave propagation analysis and supratransmission prediction of a metastable modular metastructure for non-reciprocal energy transmission,” *J. Sound Vib.*, vol. 458, October 2019.
- <sup>45</sup>J. E. Macías-Díaz and A. B. T. Motcheyo, “Energy transmission in nonlinear chains of harmonic oscillators with long-range interactions,” *Results Phys.*, vol. 18, September 2020.
- <sup>46</sup>J. Leon, “Nonlinear supratransmission as a fundamental instability,” *Phys. Lett. A*, vol. 319, pp. 130–136, December 2003.
- <sup>47</sup>J. Leon and A. Spire, “Gap soliton formation by nonlinear supratransmission in Bragg media,” *Phys. Lett. A*, vol. 327, pp. 474–480, July 2004.